Journal of Polytechnic, 2017; 20 (2) : 475-486

Performance Analysis of A Spark Ignition (SI) Otto Cycle (OC) Gasoline Engine Under Realistic Power (RP) And Realistic Power Density (RPD) Conditions

Guven GONCA*

Yildiz Technical University, Naval Arch. and Marine Eng. Depart, Besiktas, Istanbul

(Received : 13.04.2016 ; Accepted : 12.06.2016)

ABSTRACT

This study presents performance optimization of an Otto cycle (OC) gasoline engine using new criteria named as realistic power (RP) and realistic power density (RPD) conditions based on finite-time thermodynamics (FTT). The effects of design and operating parameters such as cycle temperature ratio, cycle pressure ratio, friction coefficient, engine speed, mean piston speed, stroke length, inlet temperature, inlet pressure, equivalence ratio, compression ratio and bore-stroke length ratio on the performance parameters such as effective efficiency, effective power and power density have been examined. Moreover, the energy losses have been determined as fuel's energy and they have been illustrated based on incomplete combustion, friction, heat transfer and exhaust output by using figures. Realistic values of specific heats have been used depend on temperature of working fluid. The results obtained demonstrated that the engine performance increases with increasing some parameters such as cycle temperature ratio, cycle pressure ratio, inlet pressure; with decreasing some parameters such as friction coefficient, inlet temperature. However, the engine performance could increase or decrease with respect to different conditions for some parameters such as engine speed, mean piston speed, stroke length, equivalence ratio and compression ratio. The results of this study could be used an engineering tool by Otto cycle engine designers.

Keywords: **Otto Cycle, Spark Ignition Engine, Engine Performance, Power Density, Finite-Time Thermodynamics.**

Buji Ateşlemeli Otto Çevrimli Benzinli Bir Motorun Gerçek Güç ve Gerçek Güç Yoğunluğu Koşullarında Performans Analizi

ÖZ

Bu çalışma Sonlu-Zaman Temodinamiğine dayalı olarak geliştirilen, gerçek güç ve gerçek güç yoğunluğu koşulları olarak adlandırılan yeni kriterler kullanıldığı Otto çevrimli benzinli bir motorun performans optimizasyonunu sunar. Çevrim sıcaklık oranı, çevrim basınç oranı, sürtünme katsayısı, motor hızı, ortalama piston hızı, strok uzunluğu, giriş sıcaklığı, giriş basıncı, eşdeğerlik oranı, sıkıştırma oranı ve silindir delik çapı-strok uzunluğu oranı gibi tasarım ve işletme parametrelerinin, efektif verim, efektif güç ve güç yoğunluğu üzerine etkileri incelenmiştir. Enerji kayıpları yakıt enerjisi cinsinden tanımlanmıştır ve eksik yanma, sürtünme, ısı transferi ve egzoz çıkışına dayalı olarak grafiklerle ifade edilmiştir. İş akışkanının sıcaklığına bağlı özgül ısılar kullanılmıştır. Elde edilen sonuçlar motor performansının çevrim sıcaklık oranı, çevrim basınç oranı, giriş basıncı gibi parametrelerin artışıyla arttığını; sürtünme katsayısı, giriş sıcaklığı gibi parametrelerin artışıyla azaldığını göstermiştir. Bununla birlikte, motor hızı, ortalama piston hızı, strok uzunluğu, eşdeğerlik oranı ve sıkıştırma oranı gibi parametrelerin değişimi diğer koşullara bağlı olarak performansı etkilemiştir. Bu çalışmanın sonuçları, Otto çevrimli motor tasarımı yapan tasarımcılar tarafından mühendislik aracı olarak kullanılabilir.

Anahtar Kelimeler: **Otto Çevrimi, Buji Ateşlemeli Motor, Motor Performansı; Güç Yoğunluğu; Sonlu-Zaman Termodinamiği.**

1. INTRODUCTION

Internal combustion engines (ICE) particularly, gasoline engines are commonly used by people. Due to environmental and economical restrictions, so many optimization studies have been carried out by engine designers. Mozurkewich and Berry [1] optimized the performance of an air-standard Otto cycle (ASOC) with considerations of incomplete combustion, friction loss and heat leak. Wu and Blank [2] examined the combustion effects of the OC on the work optimization and they [3] performed an optimization study with respect to engine power and mean effective pressure for the OC engine. Chen et al.[4] carried out an investigation to understand the relationship between the net work output and thermal efficiency of the ASOC taking the heat transfer losses into consideration. Wu et al. [5] applied the Miller cycle into a supercharged Otto engine to increase the net work output. Durmayaz et al. [6]

*Corresponding Author
e-mail: ggonca@yildiz.edu.tr
Digital Object Identifier (DOI) : 10.2339/2017.20.2 475-486

performed a review study on thermal systems based on FTT and thermo economics. Ge et al. [7, 8] carried out an examination on the performance of reversible [7] and irreversible [8] OC engines with consideration of variable specific heats. Chen et al. [9] determined power output and efficiency of the irreversible Otto cycle (IOC) with considerations of heat transfer losses, finite-time processes and non-isentropic processes. Ozsoysal [10] defined the heat loss as a percentage of the fuel's energy for ASOC and diesel cycle. Ge et al. [11] performed an analysis to investigate the effects of temperature-dependent specific heats and enery losses arising from friction, internal irreversibilities and heat transfer on the performance of the IOC. Hou [12] carried out a comparison about the performances of ASOC and Atkinson cycle by taking heat transfer losses into account. Abu-Nada et al. [13] conducted a thermodynamical analysis for a SI Otto engine using a new gas mixture model. Lin and Hou [14] computationally investigated the influences of variable specific heats of working fluid, heat loss and friction losses on the performance of ASOC under maximum cycle temperature conditions. Lin and Hou [15] compared the performance of ASOC and Miller cycle under the maximum temperature conditions. Wang et al. [16] examined the influences of quantum degeneracy and heat transfer between the working fluid and the cylinder wall on the optimal engine power and efficiency of an OC engine. Ust et al. [17] investigated the influences of cycle pressure and cycle temperature ratios on the performance of the IOC. Cesur et al. [18] carried out a study on a SI gasoline engine with steam injection method to examine the engine performance and exhaust emissions. Shu et al. [19] investigated the onset and severity of knocks using knock metrics in SI engine operating at various engine speeds. Gharehghani et al. [20] performed an experimental investigation on the thermal balance and performance of a turbocharged SI engine running with natural gas and they developed an empirical correlation for computing the energy of exhaust gases. Irimescu et al. [21] suggested a new procedure for estimation of blow-by rate and compression ratios based on the motored in-cylinder pressure trace for an optical SI engine. Boretti [22] examined the influences of water injection on charge efficiency, tendency to knock and temperature of exhaust gases used to operate turbo charge turbine for a turbocharged, direct injection SI engine fuelled with ethanol. Xie et al. [23] experimentally studied load controlling using EGR and spark timing for a SI engine fueled with methanol. Pan et al. [24] experimentally and theoretically examined the effects of EGR, compression ratio and boost pressure on cyclic variation of a port fuel injection (PFI) gasoline engine. Li et al. [25] carried out a study on a new hybrid breakup model to simulate the fuel injection processes of multi-hole injectors in a direct injection SI gasoline engines. Mendiburu et al. [26] investigated the performances of downdraft gasifiers integrated with gas turbine, spark and compression ignition engines for distributed power generation. Merola et al. [27] researched the influences of plasma-assisted ignition system with different plasma configurations and spark plug geometry on combustion characteristics of an optical SI engine. Pradeep et al. [28] used a compressed air injection system with LPG induction through the manifold to reduce short-circuiting losses of a two-stroke SI engine by using two different methods. Najjar et al. [29] examined the influence of variable valve lift and throat diameter on the performance and pollutant emissions of a SI engine using a computer program called Lotus which predicts gas flow, combustion and engine performance. Gurbuz et al. [30] carried out an investigation to show the effects of swirl flow on combustion parameters, cyclic variations and engine performance in a SI engine fuelled with hydrogen. Hanipah et al. [31] reviewed some of the recently reported commercial developments in free-piston engine systems particularly aimed for use in hybrid electric vehicle power trains. Wang et al. [32] placed a tumble flap into the intake port and determined the effects of it on in-cylinder aerodynamics and cycle-to-cycle variations (CCV) of direct injection SI engine using multi-cycle large-eddy simulation (LES) and proper orthogonal decomposition (POD) methods. Cucchi and Samuel [33] examined the influences of an exhaust gas turbocharger on particulate matter emissions produced by a gasoline direct injection engine. Calam et al. [34] performed a study on utilization of fusel oil in a single cylinder, SI engine and they examined the influences of the blends of gasoline and fusel oil on engine torque, specific fuel consumption and pollutant emissions at various engine speeds and loads. Wu et al. [35] simulated combustion processes of a SI natural gas engine with three kinds of different combustion chambers by using multi-dimensional computational fluid dynamics (CFD) code. Beccari et al. [36] developed two different model to predict knock onset of liquefied petroleum gas (LPG), natural gas (NG), gasoline and their mixtures in SI engines by using collected data from experiments. Gonca et al [37] carried out performance analyses and optimizations for the irreversible thermodynamic cycle engines. Bagirov et al. [38] investigated the effects of the number of injector holes on engine performance, specific fuel consumption and pollutant emissions of a gasoline engine with pre-combustion chamber. Najjar and Amer [39] used a smart device and neuro-fuzzy controller model for improving the engine volumetric efficiency, power and fuel economy of a SI engine. The results showed that the smart device improved engine power up to 21% and brake spesific fuel consumption up to 21% between 25% and 75% of engine load. However, the neuro-fuzzy controller increases engine power up to 60% and decreases the brake specific fuel consumption up to 35%.

In this study, the effects of the engine design and operating parameters on the effective efficiency, effective power and power density of an OC gasoline engine have been investigated by using a realistic

simulation model based on finite-time thermodynamics (FTT). In the literature, there is no parametrical study like this for OC gasoline engines. Apart from previous studies, a comprehensive comparison for the engine design and operating parameters has been presented. Also, energy losses with respect to exhaust output, heat transfer, friction and incomplete combustion are demonstrated as percentage of the fuel's energy. In this comprehensive report, new performance conditions have been described named as realistic power (RP) and realistic power density (RPD). Presented results could be used by real engine designer to optimize the performance of OC gasoline engines in terms of effective efficiency, effective power and power density.

2. THEORETICAL MODEL

In this study, Otto cycle (OC) engine is analyzed by using FTT model. The OC is shown in Fig. 1.

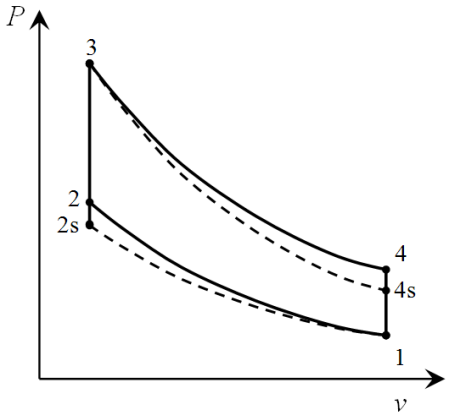

Figure 1. *P-v* diagram for the irreversible Otto cycle [48].

The parameters, constants and engine properties used in the analysis are cycle temperature ratio (α), friction coefficient (μ), residual gas fraction(RGF), engine speed (N), inlet temperature (T_1), inlet pressure (P_1), cylinder wall temperature (T_W), cylinder bore (d), stroke (L) and their standard values are given as follows: 8, 12.9 Ns/m, 0.05, 3600 rpm, 300 K, 100 kPa, 400 K, 0.072 m, 0.062 m respectively.

In the present model, the effective power, power density and efficiency are given as below:

$$P_{ef} = \dot{Q}_{in} - \dot{Q}_{out} - P_l \, , P_d = \frac{P_{ef}}{V_T} \, , \eta_{ef} = \frac{P_{ef}}{\dot{Q}_f} \tag{1}$$

Where, the total heat addition $\left(\dot{Q}_{in}\right)$ at constant volume (2-3), the total heat rejection $\left(\dot{Q}_{out}\right)$ at constant volume (4-1) and loss power by friction $\left(P_l\right)$ [11,40] could be written as below:

$$\dot{Q}_{in} = \dot{Q}_{f,c} - \dot{Q}_{ht} = \dot{m}_T \int_{T_2}^{T_3} C_V dT =$$
$$\left[\dot{m}_T \left(\begin{array}{l} 2.506 \cdot 10^{-11} \frac{T^3}{3} + 1.454 \cdot 10^{-7} \frac{T^{2.5}}{2.5} - 4.246 \cdot 10^{-7} \frac{T^2}{2} + 3.162 \cdot 10^{-5} \frac{T^{1.5}}{1.5} + \\ 1.0433T - 1.512 \cdot 10^{4} \left(-\frac{T^{-0.5}}{0.5} \right) + 3.063 \cdot 10^{5} \left(-T^{-1} \right) - 2.212 \cdot 10^{7} \left(-\frac{T^{-2}}{2} \right) \end{array} \right) \right]_{T_2}^{T_3} \tag{2}$$

$$\dot{Q}_{out} = \dot{m}_T \int_{T_1}^{T_4} C_V dT =$$
$$\left[\dot{m}_T \left(\begin{array}{l} 2.506 \cdot 10^{-11} \frac{T^3}{3} + 1.454 \cdot 10^{-7} \frac{T^{2.5}}{2.5} - 4.246 \cdot 10^{-7} \frac{T^2}{2} + 3.162 \cdot 10^{-5} \frac{T^{1.5}}{1.5} + \\ 1.0433T - 1.512 \cdot 10^{4} \left(-\frac{T^{-0.5}}{0.5} \right) + 3.063 \cdot 10^{5} \left(-T^{-1} \right) - 2.212 \cdot 10^{7} \left(-\frac{T^{-2}}{2} \right) \end{array} \right) \right]_{T_1}^{T_4} \tag{3}$$

$$P_l = \mu \bar{S}_P{}^2 = \frac{\left[Z + 48 \left(\frac{N}{1000} \right) + 0.4 \bar{S}_P{}^2 \right] V_s N}{1200} \tag{4}$$

where Z is a constant relation to friction [40] and its minimum value is taken as 75, where μ is a coefficient of friction which considers the global losses, $\bar{S}_P$ is mean piston velocity which is given as:

$$\bar{S}_p = \frac{L \cdot N}{30} \tag{5}$$

Where L and N are stroke length (m) and engine speed (rpm). $\dot{Q}_f$ is the total heat potential of the injected fuel and it is given as below:

$$\dot{Q}_f = \dot{m}_f H_u \tag{6}$$

Where H_u is lower heat value (LHV). $\dot{m}_f$ is time-dependent fuel mass and it can be expressed as follows:

$$\dot{m}_f = \frac{m_f N}{120} \tag{7}$$

Where m_f is fuel mass per cycle (kg). $\dot{Q}_{f,c}$ is heat released by combustion; $\dot{Q}_{ht}$ is the heat loss by heat transfer into cylinder wall and they are given as below:

$$\dot{Q}_{f,c} = \eta_c \dot{m}_f H_u \tag{8}$$

$$\dot{Q}_{ht} = h_{tr} A_{cyl} (T_{me} - T_W) = h_{tr} A_{cyl} \left(\frac{T_2 + T_3}{2} - T_W \right) \tag{9}$$

Where, η_c is combustion efficiency. It can be written as below [41-43]:

$$\eta_c = -1,44738 + 4,18581 / \phi - 1,86876 / \phi^2 \tag{10}$$

ϕ is equivalence ratio and it can be written as below:

$$\phi = \frac{\left(m_f / m_a \right)}{F_{st}} \tag{11}$$

Where, m_a is air mass per cycle (kg). F_{st} is stoichiometric fuel-air ratio and they are given as follows:

$$m_a = \rho_a \mathrm{V}_a = \rho_a \left(\mathrm{V}_T - \mathrm{V}_{rg} \right) \tag{12}$$

$$\mathrm{V}_T = \mathrm{V}_s + \mathrm{V}_c = \frac{(\mathrm{V}_s r)}{r-1} \tag{13}$$

$$V_c = \frac{V_T}{r} = \frac{\pi d^2 L}{4} \frac{1}{r-1} \tag{14}$$

$$F_{st} = \frac{\varepsilon \cdot (12.01 \cdot \alpha + 1.008 \cdot \beta + 16 \cdot \gamma + 14.01 \cdot \delta)}{28.85} \tag{15}$$

$$\rho_a = f(T_1, P_1) \tag{16}$$

Where V_T, V_a, V_{rg}, V_s, and V_c are volume of total cylinder, air, residual gas, stroke and clearance.

ρ_{rg} is density of residual gas which is given as below:

$$\rho_{rg} = f(T_{mix}, P_1) \tag{18}$$

T_{mix} is average temperature of air-steam mixture. They are given as below:

$$T_{mix} = \frac{\dot{m}_a T_1 R_a + \dot{m}_{rg} T_1 R_{rg}}{\dot{m}_a R_a + \dot{m}_{rg} R_{rg}} \tag{20}$$

R_a and R_{rg} are gas constants of air and residual gas. Their values are taken as 0.287kJ/kg.K

The compression ratio (r) is given as:

$$r = V_1 / V_2 \tag{21}$$

Where f stands for function. The functional expressions are obtained by using EES software [44] Where subscript "1" stands for the condition before the compression process. T_1 and P_1 are in-cylinder temperature and pressure at the beginning of compression process. T_s is the temperature of the steam injected into cylinder. Fuel used in the model is gasoline and its chemical formula is given as C_7H_{17} [45].

Where $\alpha, \beta, \gamma, \delta$ are atomic numbers of carbon, hydrogen, oxygen, nitrogen in fuel, respectively. ε is molar fuel-air ratio [45]:

$$\varepsilon = \frac{0,21}{\left(\alpha - \frac{\gamma}{2} + \frac{\beta}{4} \right)} \tag{22}$$

Where, h_{tr} is heat transfer coefficient and it is stated as [46]:

$$h_{tr} = 130 \mathrm{V}_T^{-0.06} \mathrm{P}_1^{0.8} \mathrm{T}_{mix}^{0.4} (\overline{\mathrm{S}}_p + 1.4)^{0.8} \tag{23}$$

$\dot{m}_T$, $\dot{m}_a$, $\dot{m}_{rg}$ and A_{cyl} are flow rate of total charge (kg/s), air (kg/s), residual gas (kg/s) and total heat transfer area (m^2), respectively, they are given as:

$$\dot{m}_T = \dot{m}_a + \dot{m}_f + \dot{m}_{rg}, \tag{24}$$

$$\dot{m}_a = \frac{m_a N}{120} = \frac{\dot{m}_f F_{st}}{\phi}, \tag{25}$$

$$\dot{m}_{rg} = \frac{m_{rg} N}{120} = \dot{m}_a RGF, \tag{27}$$

$$A_{cyl} = \pi d L \frac{r}{r-1} + \frac{\pi d^2}{2} \tag{28}$$

Where m_s and m_{rg} are air masses per cycle (kg). RGF is the residual gas fraction. d and r are cylinder bore (m) and compression ratio, respectively. T_{me} and T_W are mean combustion temperature and cylinder wall temperature. C_P and C_V are constant pressure and constant volume specific heats, they could be written for the temperature range of 300-3500 K as below [11]:

$$C_P = 2.506 \cdot 10^{-11} T^2 + 1.454 \cdot 10^{-7} T^{1.5} - 4.246 \cdot 10^{-7} T + 3.162 \cdot 10^{-5} T^{0.5} + 1.3301 - 1.512 \cdot 10^4 T^{-1.5} + 3.063 \cdot 10^5 T^{-2} - 2.212 \cdot 10^7 T^{-3} \tag{29}$$

$$C_V = C_P - R \tag{30}$$

The equations for reversible adiabatic processes (1-2s) and (3-4s) are respectively as follows [47]:

$$C_{V_1} \cdot \ln \left| \frac{T_{2s}}{T_1} \right| = R \ln |r| \quad , \quad C_{V_2} \cdot \ln \left| \frac{T_{4s}}{T_3} \right| = R \cdot \ln \left| \frac{1}{r} \right| \tag{31}$$

Where,

$$C_{V_1} = 2.506 \cdot 10^{-11} T_{2s1}{}^2 + 1.454 \cdot 10^{-7} T_{2s1}{}^{1.5} - 4.246 \cdot 10^{-7} T_{2s1} + 3.162 \cdot 10^{-5} T_{2s1}{}^{0.5} + 1.0433 - 1.512 \cdot 10^4 T_{2s1}{}^{-1.5} + 3.063 \cdot 10^5 T_{2s1}{}^{-2} - 2.212 \cdot 10^7 T_{2s1}{}^{-3} \tag{32}$$

$$C_{V_2} = 2.506 \cdot 10^{-11} T_{4s3}{}^2 + 1.454 \cdot 10^{-7} T_{4s3}{}^{1.5} - 4.246 \cdot 10^{-7} T_{4s3} + 3.162 \cdot 10^{-5} T_{4s3}{}^{0.5} + 1.0433 - 1.512 \cdot 10^4 T_{4s3}{}^{-1.5} + 3.063 \cdot 10^5 T_{4s3}{}^{-2} - 2.212 \cdot 10^7 T_{4s3}{}^{-3} \tag{33}$$

$$T_{2s1} = \frac{T_{2s} - T_1}{\ln \frac{T_{2s}}{T_1}} \quad T_{4s3} = \frac{T_{4s} - T_3}{\ln \frac{T_{4s}}{T_3}}, \tag{34}$$

$$\beta = P_3 / P_2 = T_3 / T_2 \tag{35}$$

β is named as pressure ratio. For irreversible conditions, T_2 and T_4 could be written as below:

$$T_2 = \frac{T_{2S} + T_1(\eta_C - 1)}{\eta_C} \quad (36)$$

$$T_4 = T_3 + \eta_E \left(T_{4S} - T_3\right) \quad (37)$$

Where η_C and η_E are isentropic efficiencies for the compression and expansion processes, respectively. In this study, the other dimensionless engine design parameters used in the analysis are cycle temperature ratio (α) and cycle pressure ratio (λ). They may be expressed respectively as:

$$\alpha = \frac{T_{max}}{T_{min}} = \frac{T_3}{T_1} = \frac{\lambda}{r} = 1 + \frac{r^{k-1} - 1}{\eta_C} \quad (38)$$

$$\lambda = P_{max} / P_{min} = P_3 / P_1 . \quad (39)$$

In the literature, energy losses could be stated as percentage of fuel's energy [14]. In this study, similar approach is used to obtain the energy losses depend on heat transfer to cylinder wall, exhaust, friction and incomplete combustion as below:

$$L_{ht} = \frac{\dot{Q}_{ht}}{\dot{Q}_{fuel}} x100 \quad , \qquad L_{ex} = \frac{\dot{Q}_{out}}{\dot{Q}_{fuel}} x100 \quad ,$$

$$L_{fr} = \frac{P_u}{\dot{Q}_{fuel}} x100 \quad , \qquad L_{ic} = \left(1 - \eta_c\right) x100 \quad (40)$$

3. RESULTS AND DISCUSSION

In this study, a new finite time thermodynamic model has been developed to evaluate effective efficiency, effective power and power density of an Otto cycle engine. Parametrical studies have been carried out to investigate the engine design and operating parameters on the performance of OC gasoline engine. The engine properties are given in Table1.

Table1. Engine properties

Engine type	Lambordini
Bore [mm]	72
Stroke [mm]	62
Cylinder Number	2
Stroke Volume [dm^3]	0.54
Maximum Power, [kW]	15
Compression ratio	10.7
Maximum speed [rpm]	3600
Cooling	Water

The variation of effective efficiency, effective power and power density are demonstrated with respect to compression ratio (r) in Figs. 2-6 and 8-13. Fig. 2 shows the effects of cycle temperature ratio on the performance parameters. The maximum effective efficiency, effective power and power density increase with increasing cycle temperature ratio owing to more energy input into cylinder. It is clear from the figure that the amplitude of power density is lower than that of effective power.

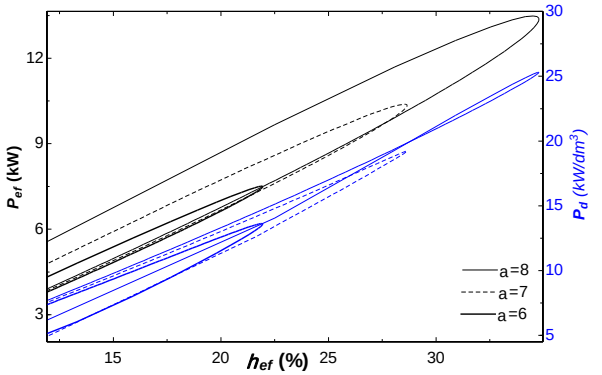

Figure 2. The variation of P_{ef} - P_d - η_{ef} with respect to α

Fig. 3 demonstrates the effects of friction coefficient on the engine performance. The friction coefficient is directly related to lubrication oil and friction surfaces. Friction losses increase with increasing the friction coefficient, hence maximum effective efficiency, effective power and power density decrease.

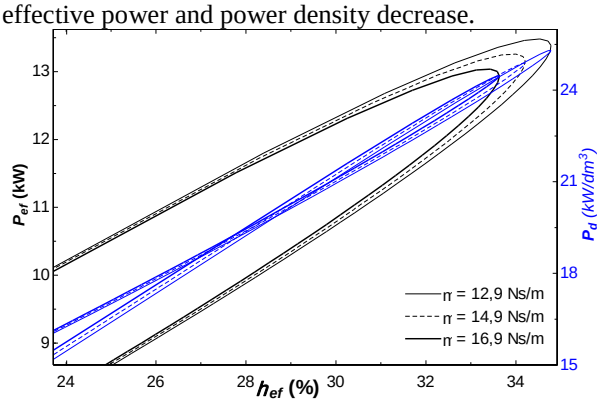

Figure 3. The variation of P_{ef} - P_d - η_{ef} with respect to μ .

Fig. 4 illustrates the effects of engine speed on the engine performance. As expected, the effective power and power density increase with increasing engine speed. However, the effective efficiency is lower at low engine speeds compared to that at high engine speeds. At high engine speeds, there are no considerable differences between maximum effective efficiencies as the friction losses increase with increasing engine speeds. It is understood that increase ratio of fuel energy given into cylinder slightly is higher compared to that of effective power and power density.

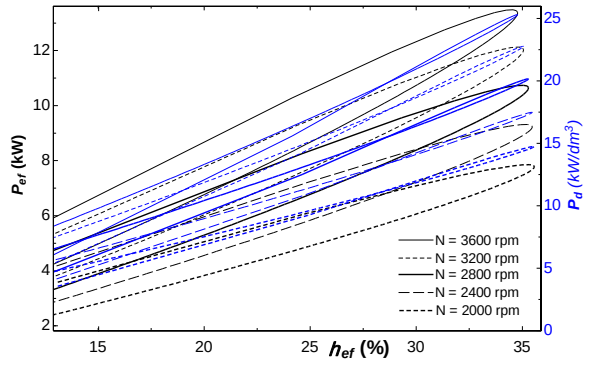

Figure 4. The variation of P_{ef} - P_d - η_{ef} with respect to N .

Fig. 5a and 5b illustrate the effects of mean piston speed on the engine performance. In these figures, two conditions are determined as constant engine speed condition (the 1. condition) and constant stroke length condition (the 2. condition). It is clear that the effective power, power density and effective efficiency increase together with increasing mean piston speed at the 1. condition since engine dimensions (stroke length and bore) enhance. However, while the effective efficiency decreases, the effective power and power density increase with increasing mean piston speed at the 2. condition as engine speed increases. It is obvious that power density change of the 2. condition is grater compared to that of 1. condition since engine dimensions increase with increasing effective power.

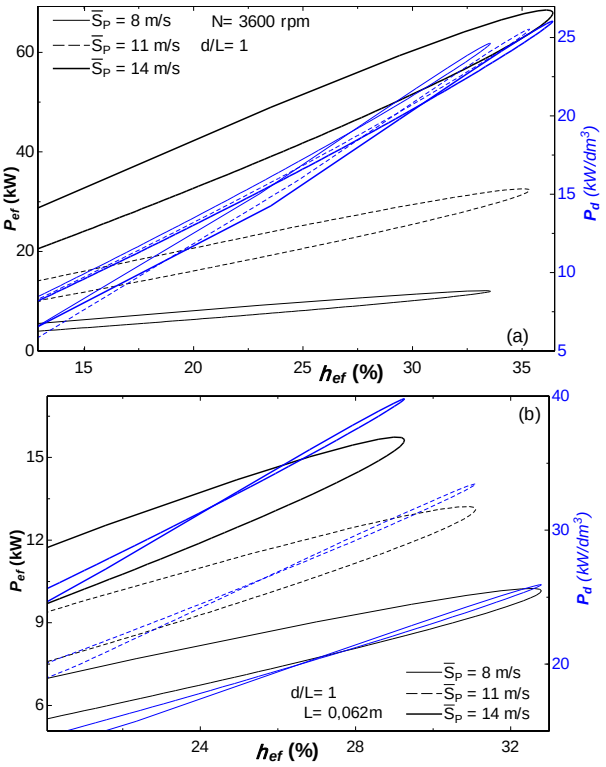

Figure 5. The variation of P_{ef} - P_d - η_{ef} with respect to $\bar{S}_p$ at constant a) N , b) L.

Fig. 6 shows the effects of stroke length on the engine performance. It is clear from the figure that the effective power increases while the effective efficiency and power density decrease with increasing stroke length. The main reason of this result is that the friction losses and engine dimensions increase with respect to stroke length. Although engine power increases, engine dimensions more increase. Also, we can see that the ratio of power change is higher than that of power density.

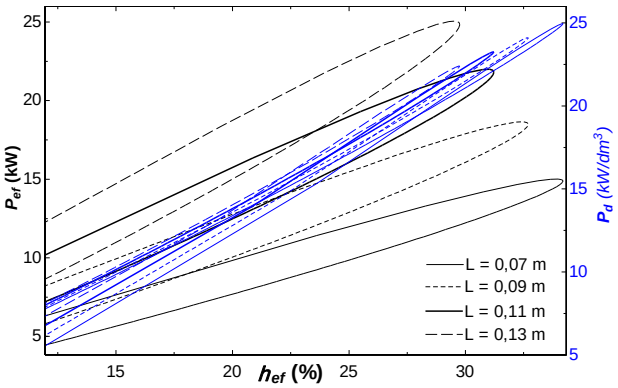

Figure 6. The variation of P_{ef} - P_d - η_{ef} with respect to L.

Figs. 7a and 7b demonstrate the effects of cycle pressure ratio and engine speed on the engine performance for constant compression ratio condition. Cycle pressure ratio has positive effect on the engine performance parameters. They increase with increasing cycle pressure ratio. The engine power and power density increase with increasing engine speed. However, the effective efficiency increases to a specified value of engine speed and then decreases. It is clear that optimum engine speed which provides the maximum effective efficiency increases with increasing cycle pressure ratio.

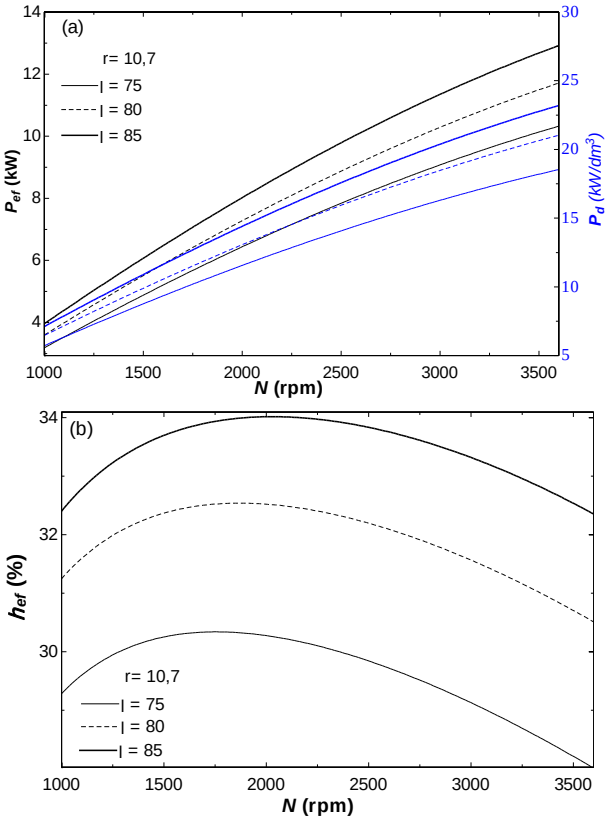

Figure 7. The variation of a) P_{ef} - P_d and b) η_{ef} with respect to N and λ .

Fig. 8a and 8b show the effects of intake temperature on the engine performance. Two main conditions have been described as constant cycle temperature ratio condition (the 1. condition) and constant maximum combustion temperature condition (the 2. condition) in these figures. At the 1. condition, the maximum effective power, power density and effective efficiency increase while intake temperature increases since maximum combustion temperature and energy input increase. However, the maximum engine performance decreases with increasing intake temperature at the 2. condition as air mass introduced into cylinder decreases.

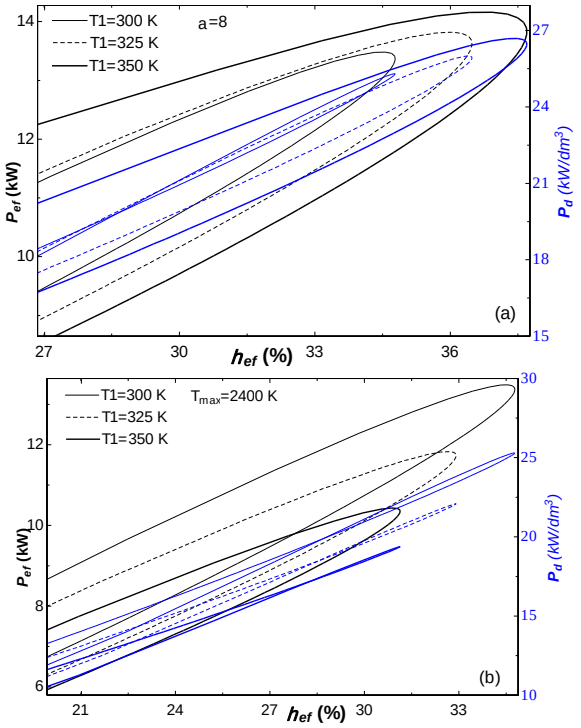

Figure 8. The variation of P_{ef} - P_d - η_{ef} with respect to T1 at constant a) α and b) T_{max}.

Fig. 9a, 9b, 9c and 9d illustrate the effects of equivalence ratio and compression ratio on the cycle temperature ratio and engine performance parameters. As can be seen from the figures, cycle temperature ratio, effective power, power density and effective efficiency increase with increasing compression ratio. However, they increase to a determined value and then begin to reduce with respect to increasing equivalence ratios. The reason for lower values of them at lower and higher equivalence ratios is that lower fuel energy input occurs at lower values of equivalence ratio. In the case of higher values of it, combustion efficiency decreases due to high rates of fuel mass input. It is clear that there are optimum values of equivalence ratio which provides maximum cycle temperature ratio, effective power, power density and effective efficiency. Their optimum values are obtained at different equivalence ratios. The maximum values of cycle temperature ratio, effective power and power density are between 1 and 1.2 of equivalence ratio while the maximum value of effective efficiency is between 0.8 and 1 of that.

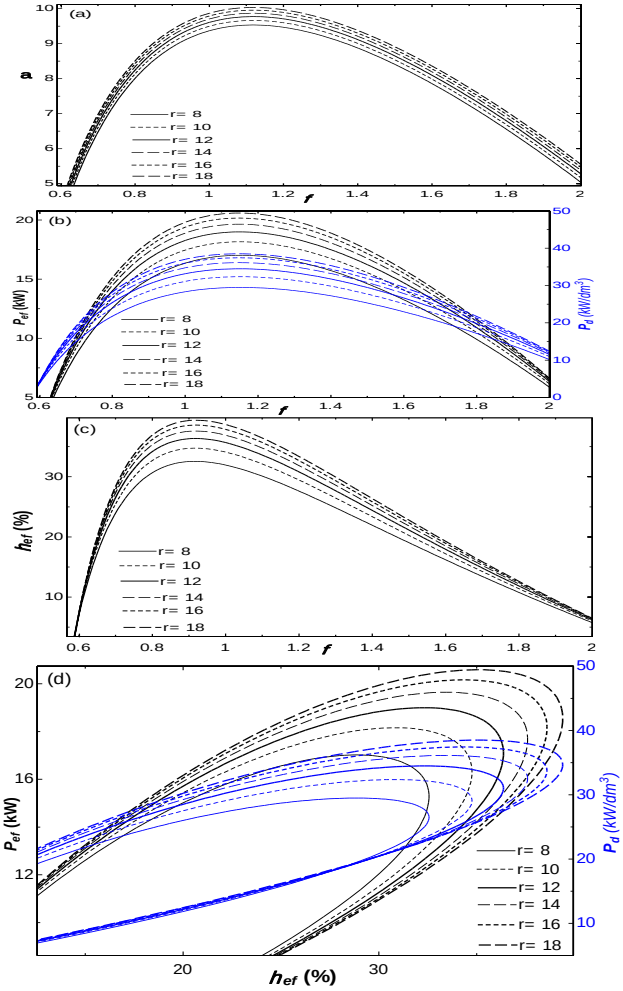

Figure 9. The variation of a) α , b) P_{ef} - P_d , c) η_{ef} and d) P_{ef} - η_{ef} with respect to r and ϕ .

Fig. 10 shows the influence of equivalence ratio on the engine performance. Similar to previous figures, the maximum effective efficiency, effective power and power density increase to particular values of equivalence ratio and then start to decrease. The maximum effective efficiency is seen when equivalence ratio is equal to 0.9 while the maximum effective power is seen when equivalence ratio happens 1.2.

The effects of cylinder wall temperature on the engine performance is shown in Fig.11. There are no considerable changes in maximum effective power and power density depend on cylinder wall temperature. However, maximum effective efficiency increases with increasing cylinder wall temperature as heat transfer loss decreases.

Fig.12 demonstrates the influence of intake pressure on the engine performance. It is known that more air mass is introduced into the cylinder at higher pressure conditions.

Therefore, engine performance raises with increasing intake pressure.

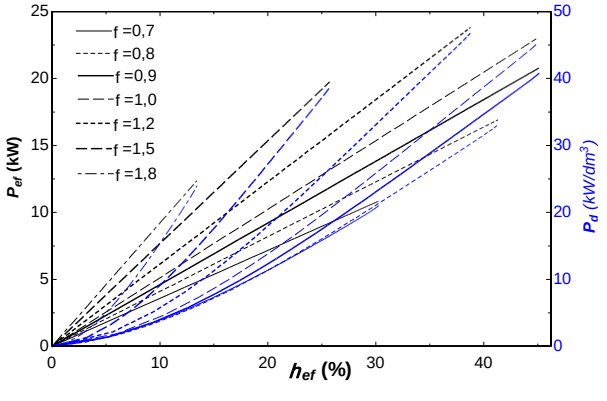

Figure 10. The variation of P_{ef} - P_d - η_{ef} with respect to ϕ.

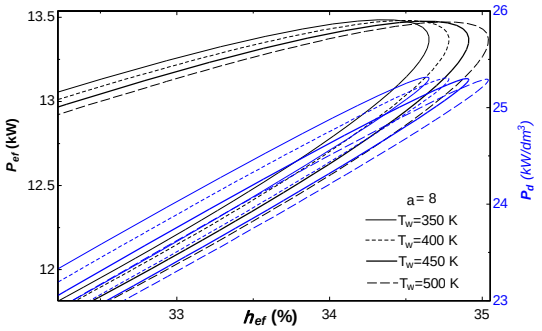

Figure 11. The variation of P_{ef} - P_d - η_{ef} with respect to T_W.

.

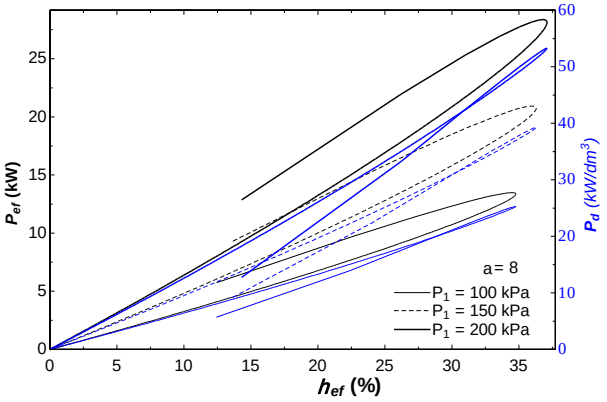

Figure 12. The variation of P_{ef} - P_d - η_{ef} with respect to P_1.

The influence of ratio of bore to stroke length (d/L) on the engine performance is shown in Fig.13. It is obvious that the engine performance increases with increasing d/L owing to increasing engine dimensions.

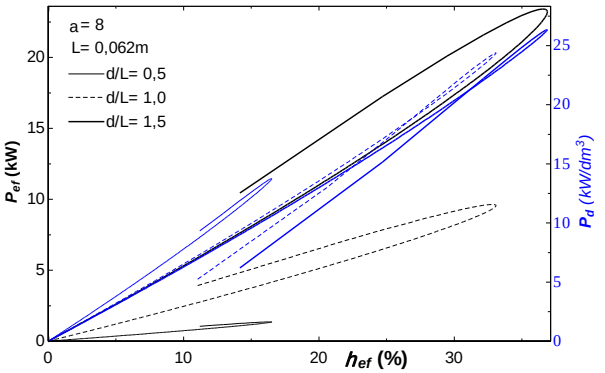

Figure 13. The variation of P_{ef} - P_d - η_{ef} with respect to d/L.

Fig. 14 shows the effects of d/L on the engine performance at constant cylinder volume for different conditions. In this figures, three conditions are determined as constant cycle temperature ratio and stroke length condition (the 1. condition); constant equivalence ratio and stroke length condition (the 2. condition); constant equivalence ratio and compression ratio condition (the 3. condition). At the 1. condition, the effective power, power density and effective efficiency increase to a specified value and then begin to abate with increasing d/L. At the 2. and 3. conditions, the effective power, power density and effective efficiency raise with increasing d/L.

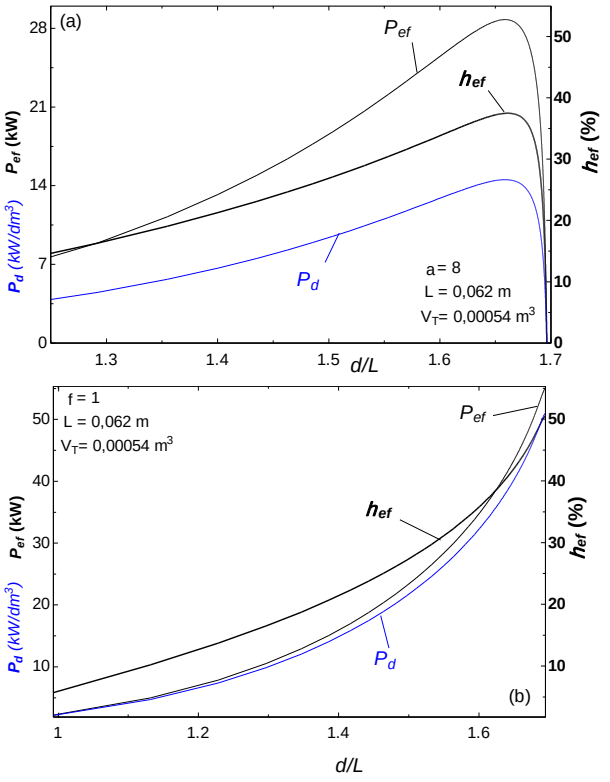

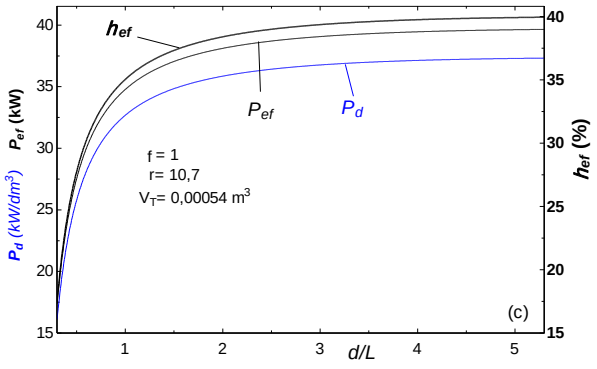

Figure 14. The effects of d/L on P_{ef} - P_d - η_{ef} variation at constant a) α and L, b) ϕ and L, c) ϕ and r.

Fig. 15 illustrate the effects of compression ratio on losses as fuel's energy. In order to investigate the energy losses, two conditions are determined as constant cycle temperature ratio condition (the 1. condition) and constant equivalence ratio condition (the 2. condition). Incomplete combustion loss (L_{ic}) and heat transfer loss (L_{ht}) increase whilst exhaust energy loss (L_{ex}) decreases and friction loss (L_{fr}) remains constant with increasing compression ratio at the 1. condition. Total cylinder volume and equivalence ratio change with respect to changing of compression ratio at this condition. However, L_{ic} and L_{fr} are constant, L_{ht} increases and L_{ex} decreases with respect to increasing compression ratio at the 2. condition. L_{ic} does not change at constant equivalence ratio because combustion efficiency is constant. Total cylinder volume increases with increasing compression ratio, hence L_{ht} increases and L_{ex} decreases. L_{fr} changes with respect to stroke length and engine speed which are constant at both of the conditions. Therefore, L_{fr} does not change at the 2. condition due to constant fuel energy input. At the 1. condition, it increases since fuel energy input decreases with increasing compression ratio.

4. CONCLUSION

In this study, the effects of the engine design and operating parameters on the effective power, power density and effective efficiency of an OC gasoline engine have been examined by using a realistic model based on the FTT. A comprehensive parametrical study has been carried out. In the parametrical studies, the effects of cycle temperature ratio (α), cycle pressure ratio (λ), friction coefficient (μ), engine speed (N), mean piston speed ($\overline{S}_p$), stroke length (L), inlet temperature (T1), inlet pressure (P1), equivalence ratio (ϕ), compression ratio (r) and bore-stroke length ratio (d / L) on the effective power, power density and effective efficiency have been examined. The results show that the effective power, power density and effective efficiency increase with increasing cycle temperature ratio (α), cycle pressure ratio (λ), inlet pressure (P1).

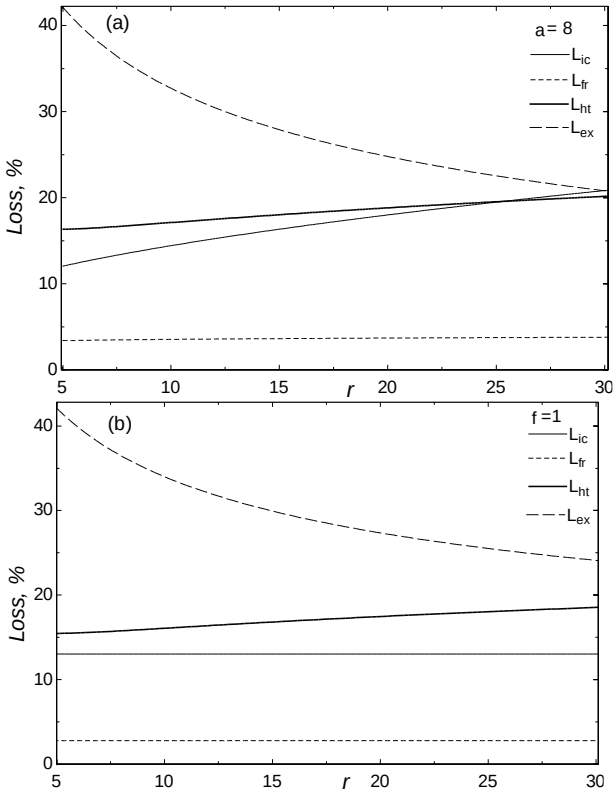

Figure 15. The variation of energy loss percentages with respect to r for constant a) α and b) ϕ .

The engine performance decreases with friction coefficient (μ). On the other hand, the effective power, power density and effective efficiency increase with increasing mean piston speed for constant engine speed conditions, however, as the effective power and power density increase, the effective efficiency decreases with increasing mean piston speed for constant stroke length conditions. While the effective power and power density increase, the effective efficiency decreases with increasing stroke length and engine speed. The effective power, power density and effective efficiency increase up to a determined value and then start to decrease with increasing equivalence ratio and compression ratio. The energy losses with respect to incomplete combustion and heat transfer increase, as exhaust output losses decreases with increasing compression ratio for constant α conditions. At this condition, friction losses are constant. However, the losses depend on friction and incomplete combustion are constant, while exhaust output losses decrease and heat transfer losses increase at the constant equivalence ratio conditions. The results are scientifically valuable and therefore, they can be assessed by gasoline engine designers.

Nomenclature

A	heat transfer area (m^2)
ASOC	Air-standard Otto cycle
C_v	constant volume specific heat (kJ/kg.K)
C_p	constant pressure specific heat (kJ/kg.K)
d	bore (m)
F	fuel-air ratio
FTT	finite-time thermodynamic
h_{tr}	heat transfer coefficient (W/ m^2K)
H_u	lower heat value of the fuel (kJ/kg)
ICE	Internal combustion engines
IOC	Irreversible Otto cycle
l	loss
L	stroke length (m), energy loss percentage (%)
m	mass (kg)
$\dot{m}$	time- dependent mass rate (kg/s)
N	engine speed (rpm)
OC	Otto cycle
P	pressure (bar), power (kW)
$\dot{Q}$	rate of heat transfer (kW)
r	compression ratio
R	gas constant (kJ/kg.K)
RGF	residual gas fraction
RP	realistic power
RPD	realistic power density
S	stroke (m)
$\overline{S}_P$	mean piston speed (m/s)
T	temperature (K)
v	specific volume (m^3/kg)
V	volume (m^3)

Greek letters

α	cycle temperature ratio, atomic number of carbon
β	pressure ratio, atomic number of hydrogen
δ	atomic number of nitrogen
ϕ	equivalence ratio
γ	atomic number of oxygen
λ	cycle pressure ratio
μ	friction coefficient (Ns/m)
ρ	density (kg/m^3)
η_C	Isentropic efficiency of compression
η_E	Isentropic efficiency of expansion

Subscripts

1	at the beginning of the compression process
a	air
c	combustion, clearance
cyl	cylinder
ef	effective
f	fuel
fr	friction
ht	heat transfer
i	initial condition
ic	incomplete combustion
in	input
l	loss
max	maximum
me	mean
min	minimum
mix	mixture
out	output
rg	residual gas
s	stroke, isentropic condition
st	stoichiometric
t	total
w	cylinder walls

REFERENCES

[1] Mozurkewich M. and Berry R. S., "Optimal Paths for Thermodynamic Systems: The Ideal Otto Cycle", ***J. Appl. Phys.***, 53(1): 34–42, (1982).

[2] Wu C. and Blank D. A., "The Effects Of Combustion on a Work-Optimized Endoreversible Otto Cycle", ***J. Inst. Energy***, 65: 86–89, (1992).

[3] Wu C. and Blank D. A., "Optimization of the Endoreversible Otto Cycle with Respect to Both Power and Mean Effective Pressure", ***Energy Convers. Manage.***, 34: 1255–1259, (1993).

[4] Chen L., Wu C., Sun F. and Caoi S., "Heat Transfer Effects on the Net Work Output and Efficiency Characteristics For An Air standard Otto Cycle", ***Energy Convers. Manage.,*** 39: 643–648, (1998).

[5] Wu C., Puzinauskas P. V. and Tsai J. S., "Performance analysis and optimization of a supercharged Miller cycle Otto engine", ***Appl. Therm. Eng.,*** 23: 511-521, (2003).

[6] Durmayaz A., Sogut O. S., Sahin B. and Yavuz H., "Optimization of thermal systems based on finite-time thermodynamics and thermoeconomics", ***Prog. Energ. Combust. Sci.,*** 30: 175–217, (2004).

[7] Ge Y., Chen L., Sun F. and Wu C., "Thermodynamic Simulation of Performance of an Otto Cycle with Heat Transfer and Variable Specific heats for the Working Fluid", ***Int. J. Therm. Sci.,*** 44(5): 506–511, (2005).

[8] Ge Y., Chen L., Sun F. and Wu C., "The Effects of Variable Specific-Heats of the Working Fluid on the Performance of an Irreversible Otto cycle", ***Int. J. Exergy,*** 2(3): 274–283, (2005).

[9] Chen J., Zhao Y. and He J., "Optimization Criteria for the Important Parameters of an Irreversible Otto Heat-Engine", ***Appl. Energy,*** 83: 228-238, (2006).

[10] Ozsoysal O. A., "Heat Loss as a Percentage of the Fuel's Energy in Air Standard Otto and Diesel Cycles", ***Energy Convers. Manage.,*** 47(7-8): 1051–1062, (2006).

[11] Ge Y., Chen L., Sun F. and Wu C., "Finite-Time Thermodynamic Modelling and Analysis of an Irreversible Otto-Cycle", ***Appl. Energy,*** 85: 618-624, (2008).

[12] Hou S. S., "Comparison of the Performances of Air Standard Atkinson and Otto Cycles with Heat-Transfer Considerations", ***Energy Convers. Manage.,*** 48(5): 1683–1690, (2007).

[13] Abu-Nada E., Al-Hinti I., Akash B. and Al-Sarkhi., "Thermodynamic analysis of spark-ignition engine using a gas mixture model for the working fluid", ***Int. J. Energy Res.*** 31: 1031–1046, (2007).

[14] Lin J. C. and Hou S. S., "Effects of Heat Loss As Percentage of Fuel's Energy, Friction And Variable Specific Heats Of Working Fluid On Performance of Air Standart Otto Cycle", ***Energy Convers. Manage.,*** 49: 1218–1227, (2008).

[15] Lin J. C and Hou S. S., "Performance analysis of an air-standard Miller cycle with considerations of heat loss as a percentage of fuel's energy, friction and variable specific heats of working fluid", ***Int. J. Therm. Sci.,*** 47: 182–191, (2008).

[16] Wang H., Liu S. and He J., "Performance analysis and parametric optimum criteria of a quantum Otto heat engine with heat transfer effects", ***Appl. Therm. Eng.,*** 29: 706-711, (2009).

[17] Ust Y., Sahin B. and Safa A., "The Effects of Cycle Temperature and Cycle Pressure Ratios on the Performance of an Irreversible Otto Cycle", ***Acta Phys. Pol. A,*** 120: 412–416, (2011).

[18] Cesur I., Parlak A,. Ayhan V., Gonca G. and Boru B., "The effects of electronic controlled steam injection on spark ignition engine", ***Appl. Therm. Eng.,*** 55: 61–68, (2013).

[19] Shu G., Pan J. and Wei H., "Analysis of onset and severity of knock in SI engine based on in-cylinder pressure oscillations", ***Appl. Therm. Eng.,*** 51(1-2): 1297-1306, (2013).

[20] Gharehghani A., Koochak M., Mirsalim M. and Yusaf T., "Experimental investigation of thermal balance of a turbocharged SI engine operating on natural gas", ***Appl. Therm. Eng.*** 60(1-2): 200-207, (2013).

[21] Irimescu A., Tornatore C., Marchitto L. and Merola S. S., "Compression ratio and blow-by rates estimation based on motored pressure trace analysis for an optical spark ignition engine", ***Appl. Therm. Eng.,*** 61(2): 101-109, (2013).

[22] Boretti A., "Water injection in directly injected turbocharged spark ignition engines", ***Appl. Therm. Eng.,*** 52: 62-68, (2013).

[23] Xie F. X., Li X. P., Wang X.C., Su Y. and Hong W., "Research on using EGR and ignition timing to control load of a spark-ignition engine fueled with methanol", ***Appl. Therm. Eng.,*** 50(1): 1084-1091, (2013).

[24] Pan M., Shu G., Wei H., Zhu T., Liang Y. and Liu C., "Effects of EGR, compression ratio and boost pressure on cyclic variation of PFI gasoline engine at WOT operation", ***Appl. Therm. Eng.,*** 64(1-2): 491-498, (2014).

[25] Li Z. H., He B. Q. and Zhao H., "Application of a hybrid breakup model for the spray simulation of a multi-hole injector used for a DISI gasoline engine", ***Appl. Therm. Eng.*** 65(1-2): 282-292, (2014).

[26] Mendiburu A. Z., Roberts J. J., Carvalho J. A. and Silveira J. L., "Thermodynamic analysis and comparison of downdraft gasifiers integrated with gas turbine, spark and compression ignition engines for distributed power generation", ***Appl. Therm. Eng.*** 66(1-2): 290-297, (2014).

[27] Merola S. S., Marchitto L., Tornatore C., Valentino G. and Irimescu A., "Optical characterization of combustion processes in a DISI engine equipped with plasma-assisted ignition system", ***Appl. Therm. Eng.*** 69(1-2): 177-187, (2014).

[28] Pradeep V., Bakshi S. and Ramesh A., "Scavenging port based injection strategies for an LPG fuelled two-stroke spark-ignition engine", ***Appl. Therm. Eng.,*** 67(1-2): 80-88, (2014).

[29] Najjar Y. S. H., Ghazal O. H. and AL-Khishali K. J. M., "Performance improvement of green cars by using variable-geometry engines", ***J. Energy Ins.,*** 87(4): 393-400, (2014).

[30] Gürbüz H., Akçay I. H. and Buran D., "An investigation on effect of in-cylinder swirl flow on performance, combustion and cyclic variations in hydrogen fuelled spark ignition engine", ***J. Energy Ins.,*** 87(1): 1-10, (2014).

[31] Hanipah M. R., Mikalsen R. and Roskilly A. P., "Recent commercial free-piston engine developments for automotive applications", ***Appl. Therm. Eng.,*** 75: 493-503, (2015).

[32] Wang T., Li W., Jia M., Liu D., Qin W. and Zhang X., "Large-eddy simulation of in-cylinder flow in a DISI engine with charge motion control valve: Proper orthogonal decomposition analysis and cyclic variation", ***Appl. Therm. Eng.*** 75: 561-574, (2015).

[33] Cucchi M. and Samuel S., "Influence of the exhaust gas turbocharger on nano-scale particulate matter emissions from a GDI spark ignition engine", ***Appl. Therm. Eng.*** 76: 167-174, (2015).

[34] Calam A., Solmaz H., Uyumaz A., Polat S., Yilmaz E and İçingür Y., "Investigation of usability of the fusel oil in a single cylinder spark ignition engine", ***J. Energy Ins.,*** 88(3): 258-265, (2015).

[35] Wu C., Deng K. and Wang Z., "The effect of combustion chamber shape on cylinder flow and lean combustion process in a large bore spark-ignition CNG engine", ***J. Energy Ins.,*** 89(2): 240-247, (2016).

[36] Beccari S., Pipitone E. and Genchi G., "Knock onset prediction of propane, gasoline and their mixtures in

spark ignition engines", ***J. Energy Ins.,*** 89(1): 101-114, (2016).

[37] Gonca G., Sahin B., Ust Y. and Parlak A., "Comprehensive performance analyses and optimization of the irreversible thermodynamic cycle engines (TCE) under maximum power (MP) and maximum power density (MPD) conditions", ***Appl. Therm. Eng.*** 85: 9-20, (2015).

[38] Bagirov H., Can I., Oner C., Sugozu I. and Kapicioglu A., "Experimental investigation the effects of mixture impoverished on the specific fuel consumption, engine performance and exhaust emissions a pre-combustion chamber gasoline engine", ***J. Energy Ins.,*** 88(3): 205-208, (2015).

[39] Najjar Y. S. H. and Amer M. M. B., "Using a smart device and neuro-fuzzy control system as a sustainable initiative with green cars", ***J. Energy Ins.,*** 89(2): 256-263, (2016).

[40] Gonca G., Sahin B., Ust Y. and Parlak A., "A Study on Late Intake Valve Closing Miller Cycled Diesel Engine", ***Arab. J. Sci. Eng.,*** 38: 383-293, (2013).

[41] Ebrahimi R., "Performance analysis of an irreversible Miller cycle with considerations of relative air–fuel ratio and stroke length", ***Appl. Math. Model.,*** 36: 4073-4079, (2012).

[42] Ebrahimi R., "Thermodynamic modeling of performance of a Miller cycle with engine speed and variable specific heat ratio of working fluid", ***Computers and Mathematics with Applications***, 62: 2169-2176, (2011).

[43] Ebrahimi R., "Effects of mean piston speed, equivalence ratio and cylinder wall temperature on performance of an Atkinson engine", ***Mathematical and Computer Modelling***, 53: 1289-1297, (2011).

[44] EES Academic Professional Edition, V.9.701-3D, USA, ***F-Chart Software***, (2014).

[45] Ferguson C. R., "Internal combustion engines – applied thermosciences", ***John Wiley & Sons Inc.,*** New York, (1986).

[46] Hohenberg G. "Advanced Approaches for Heat Transfer Calculations", ***SAE,*** 790-825, (1979).

[47] Lin J., Chen L., Wu C. and Sun F., "Finite-Time Thermodynamic Performance of a Dual Cycle", ***Int. J. Energy Res.,*** 23(9): 765–772, (1999).

[48] Gonca G., "Effects of engine design and operating parameters on the performance of a spark ignition (SI) engine with steam injection method (SIM)", ***Appl. Math. Model.,*** In press., (2017).